Climate Dynamics (2003) 20: 723–739
DOI 10.1007/s00382-003-0304-x

E. Xoplaki · J. F. González-Rouco · J. Luterbacher
H. Wanner

Mediterranean summer air temperature variability and its connection to the large-scale atmospheric circulation and SSTs

Received: 27 August 2002 / Accepted: 13 December 2002 / Published online: 13 March 2003

Abstract The interannual and decadal variability of summer (June to September) air temperature over the Mediterranean area is analyzed for the period 1950 to 1999. The combined influence of the large-scale atmospheric circulation at different levels and thermic predictors (thickness patterns and Mediterranean SSTs) on station temperature data is assessed by means of optimal objective techniques. The validity of the statistical models has been evaluated through cross-validation. Three large-scale predictor fields (300 hPa geopotential height, 700–1000 hPa thickness and SSTs) account for more than 50% of the total summer temperature variability. The positive phase of the first canonical mode is associated with blocking conditions, subsidence and stability related to warm Mediterranean summers. The second CCA mode shows an east–west dipole of the Mediterranean summer air temperature connected by a combination of a trough as well as an extended ridge over the western and eastern parts of the Mediterranean, respectively. Though both modes are found to contribute to long-term summer temperature trends in the 1950–1999 period, it is shown that the first canonical mode is mainly responsible for the 0.4 °C warming (significant at the 95% level) over the last 50 years of the twentieth century. Further, the analysis reveals that the Mediterranean summer temperatures were higher in the 1860s, 1950s and 1990s and lower around 1910 and in the 1970s. A significant temperature increase of 0.5 °C (0.27 °C) is found for the 1900–1999 (1850–1999) period.

E. Xoplaki (✉) · J. Luterbacher · H. Wanner
Institute of Geography,
University of Bern, Hallerstrasse 12,
3012 Bern, Switzerland
E-mail: elena.xoplaki@giub.unibe.ch

E. Xoplaki
Department of Meteorology and Climatology,
University of Thessaloniki, Greece

J. F. González-Rouco
Departamento de Astrofísica y Ciencias de la Atmósfera,
Universidad Complutense de Madrid, Spain

J. Luterbacher · H. Wanner
NCCR Climate, University of Bern,
Switzerland

1 Introduction

Ecological systems, human health and socio-economic sectors, all of which are vital for sustainable development, are sensitive to climate change (Watson et al. 1997). Quantifying and understanding climatic changes at the regional scale is one of the most important and uncertain issues within the global change debate. Until the present, projections of regional climate changes for the twenty first century have been based on coupled atmosphere–ocean general circulation model (AOGCM) simulations of the climate system response to changes in anthropogenic forcings (e.g. Kattenberg et al. 1996; Cubasch et al. 2001).

A step towards the understanding of regional climatic changes and impacts is the assessment of the characteristics of natural climate variability and of the AOGCM performance in reproducing it (Giorgi 2002a,b). Climate variability can mask man-made forced signals, so that a characterization of the natural variability is necessary to evaluate the intensity of the forced change signal.

A large number of previous studies described trends and variability through a wide range of scales, from the global to the local (e.g. Nicholls et al. 1996; Jones et al. 1999; Easterling et al. 2000; Hansen et al. 2001, 2002; Folland et al. 2001; New et al. 2001). The structure of climate series can differ considerably across regions and locations showing variability at a range of scales in response to changes in the direct radiative forcing and variations in internal modes of the climate system (New et al. 2001; Hansen et al. 2001; Giorgi 2002a).

Mediterranean climate constitutes an issue of particular concern within the context of regional climate

variability and change. The IPCC (2001) has shown that higher maximum temperatures and more hot days are likely to increase in frequency during the twenty first century. Over the last few decades, extended heat waves and droughts appear to have become more frequent in the Mediterranean (IPCC 2001). These can have disastrous consequences on natural ecosystems and several aspects of society like health or economic wealth: heat waves cause rises in the death rate, especially in urban areas (e.g. July/August 1983, July 1987, 1988 in Greece, 1998 in Cyprus, Katsouyanni et al. 1988, 1993; Giles and Balafoutis 1990; Giles et al. 1990; Matzarakis and Mayer 1991, 1997; Perry 2001); soil degradation may force migration, an issue of great concern particularly in the southern Mediterranean area; prolonged droughts and water supply problems and fires might weaken tourist inflows to the Mediterranean (Kundzewicz et al. 2001; Tsiourtis 2001). The extent and severity of desertification, water shortage and water quality, food security, risks in public health, sensitivity of valuable ecosystems and indirect effects on national economies are some of the topics indicating the vulnerability of the Mediterranean basin to climate variability.

Fluctuations and changes in atmospheric circulation are important elements of the climate. Namias (1948) was among the first to state that the mean monthly geopotential height fields for mid tropospheric levels determine monthly air temperature anomalies. Therefore, advective processes exerted by the atmospheric circulation are a crucial factor controlling the regional air temperature changes (e.g. Trenberth 1990, 1995; Xu 1993; Hurrell 1995; Hurrell and van Loon 1997; Slonosky et al. 2001; Xoplaki et al. 2000, 2002; Jacobeit et al. 2001; Pozo-Vázquez et al. 2001; Slonosky and Yiou 2002; Xoplaki 2002).

The Mediterranean basin and the surrounding lands are influenced by some of the most relevant mechanisms acting upon the global climate system. It marks a transitional zone between the deserts of North Africa situated within the arid zone of the subtropical high and Central and Northern Europe affected by the westerly flow during the whole year. In addition, the Mediterranean climate is exposed to the South Asian Monsoon in summer, the Siberian High Pressure System in winter, the El Niño Southern Oscillation and the North Atlantic Oscillation (e.g. Corte-Real et al. 1995; Maheras 2000; Ribera et al. 2000). The main physical and geographical factors controlling the spatial distribution of the climatic conditions over the Mediterranean are the atmospheric circulation, the latitude, the altitude and generally the orography, the land–sea interactions (distance from the sea) and smaller scale processes (Lolis et al. 1999; Xoplaki et al. 2000; Xoplaki 2002). The size, position, and configuration of the Mediterranean produce a variety of local modifications that ranges from desert to humid mountain climates.

Mediterranean climate is also influenced by the almost enclosed Mediterranean Sea itself. It represents an important source of energy and moisture for cyclone development and its complex land topography plays a crucial role in steering air flow (Bartzokas et al. 1994; Trigo et al. 1999; Maheras et al. 2001).

Mediterranean summers are warm and mostly dry in a large part of the basin. This can be mainly attributed to a strong high pressure ridge extending from the Azores subtropical high. Over Egypt, this ridge is displaced southward by a trough extending northwest from the Arabian Gulf towards Greece, which is associated with the Indian summer monsoon depression (Palutikof et al. 1996).

Giorgi (2002a) analyzed the winter, summer and yearly air temperature variability and trends over the larger Mediterranean land-area (averaged over the grid points 30°N–48°N and 20°W–40E) for the period 1901–1998 based on the gridded (0.5°×0.5° latitude–longitude) data set of New et al. (1999, 2000). He found a statistically significant annual warming trend over the larger Mediterranean land-area of around 0.75 °C (1901–1998), mostly from contributions in the early and late decades of the century. Slightly higher values were obtained for winter and summer. This is in agreement with the findings of the IPCC (Folland et al. 2001). Based on the same gridded data (New et al. 1999, 2000), Jacobeit (2000) found a significant overall summer warming over the entire Mediterranean for the period 1969–1998.

It has also been proposed that sea surface temperature (SST) anomalies govern, at least partly, precipitation and air temperature anomalies in neighboring continental regions (Hunt and Gordon 1988; Zorita et al. 1992; Reddaway and Bigg 1996; Rimbu et al. 2001; Xoplaki 2002; Xoplaki et al. 2002). In addition, there are strong indications that fluctuations in SST, and hence fluctuations of surface fluxes, are intimately involved in decadal-scale climate variability (Trigo et al. 2000).

Many studies have been published relating changes in Mediterranean air temperature regimes to the large-scale atmospheric circulation (Corte-Real et al. 1995, 1998; Reddaway and Bigg 1996; Hurrell and van Loon 1997; Kutiel and Maheras 1998; Maheras et al. 1999; Saenz et al. 2001; Kutiel and Benaroch 2002; Xoplaki 2002; Xoplaki et al. 2002). Parts of these papers have evaluated the fraction of air temperature variability explained by major sea level pressure (SLP) and/or upper-air large-scale anomalies. Other studies analyzed the air temperature variability patterns over a specific geographical area in the Mediterranean and identified the surface and upper-air large-scale anomalies such as the North Atlantic Oscillation, the Eastern Atlantic pattern, the Scandinavian pattern, the Eurasian pattern (Barnston and Livezey 1987) and the El Niño Southern Oscillation.

To determine the cause of the observed changes in Mediterranean air temperature over the last few decades needs improved understanding of the origin of the atmospheric circulation changes as well as the influence of the state of the SSTs. Instead of relating one single field to explain spatial climate variability, it is more appropriate to combine information from various large-scale climate fields in order to account for stronger relations and a higher amount of air temperature and

precipitation variability over a given area. Xoplaki et al. (2002) showed that the combination of eight large-scale predictor fields including SLP, geopotential height fields at different levels, thickness and Mediterranean SST fields explain more of the total summer air temperature variability over Greece and western Turkey than using a single field alone.

In this study, we extend our analysis over the entire Mediterranean to improve our understanding of interannual and decadal variability of Mediterranean summer air temperature for the period 1950–1999. The simultaneous relationship between the combined information of large-scale atmospheric circulation at various levels and SSTs is directly assessed with an optimal methodology. Hundreds of series of monthly surface air temperature measurements, quality checked and homogenized, will be used in combination with reanalysis data and SST fields.

In Sects. 2 and 3, the data sets and the multivariate methods are briefly described. Section 4 includes the results related to the combined information of large-scale anomaly fields of SLP, geopotential height fields, thickness patterns and SSTs to Mediterranean summer air temperature through canonical correlation analysis (CCA) in the empirical orthogonal function (EOF) space. The discussion and the conclusions are presented in Sects. 5 and 6, respectively.

2 Data

The following data sets have been used in this study: (1) gridded (2.5°×2.5° latitude–longitude resolution) SLP data, geopotential heights at different levels (1000 hPa, 850 hPa, 700 hPa, 500 hPa and 300 hPa) and gridded (T62 Gaussian grid) air temperature at 2 m height were taken from the NCEP/NCAR reanalysis data sets (Kalnay et al. 1996; Kistler et al. 2001). Monthly mean values were computed from the 6-hourly data. Thickness fields (300–500 hPa; 500–700 hPa and 1000–700 hPa) were derived from the corresponding geopotential height data. The monthly SST data were taken from the Global Sea Ice Surface Temperature, version 2.3b (GISST2; spatial resolution is 1°×1° latitude–longitude) dataset (Rayner et al. 1996, updated). (2) Monthly station series of air temperature for the area 25°–48°N and 10°W–45°E including 30 countries along or close to the Mediterranean Sea were collected and digitized. The data were obtained mainly from the various National Meteorological services or other official institutions. For countries that did not provide any data, the GHCN (Global Historical Climatology Network) version 2 air temperature data have been used, which are extensively quality controlled (Vose et al. 1992; Peterson and Vose 1997; Peterson et al. 1998; for a detailed discussion of the GHCN v2 data the reader is referred to: http://cdiac.esd.ornl.gov/ghcn/ghcn.html#over2).

From 1901 to the end of the 1940s the Mediterranean areas are characterized by poor station coverage, especially over Northern Africa and the eastern basin. Around 1950 there is a sharp increase in the number of stations, which were mainly due to the inclusion of the 1951–1960 version of the World Weather Records dataset in the World Monthly Surface Station Climatology (Dai et al. 1997) Therefore, the analysis is restricted to the 50 year period 1950–1999 with a spatially homogeneous station distribution of 247 air temperature series over the larger Mediterranean area.

The selected period of our analysis covers the summer months June 1950 to September 1999 for air temperature. Figure 1 shows the distribution of stations with continuous monthly records of air temperature for the period 1950–1999. Homogenized series are marked with triangles, quality controlled (according to the guidelines of the World Meteorological Organization (WMO 1986)) with circles and GHCN v2 series with crosses. In order to isolate the characteristics of the atmospheric variability regarding the larger Mediterranean area, a spatial window was selected, based on the highest correlation between the first principal component (PC) of the Mediterranean summer air temperature and the large-scale Northern Hemisphere geopotential height fields. The geographical area spanning from 60°W to 80°E and 10°N to 80°N, including 1653 grid points, provides the most valuable atmospheric information concerning summer air temperature over the Mediterranean area. To relate SST to the Mediterranean summer air temperature, a spatial window (with 1100 grid points) covering the entire Mediterranean and the Black Sea (9.5°W–44.5°E, 30.5°–49.5°N) was chosen.

3 Methodology

Canonical correlation analysis in empirical orthogonal function space is used to investigate the connection between the large-scale climate states and the summer air temperature variability. The CCA is an appropriate method to search for the linear relationship between two space/time dependent variable sets. The CCA selects pairs of spatial patterns of each variable set such that the (time dependent) pattern amplitudes are optimally correlated. The canonical time series describe the strength and the sign of the corresponding pattern for each realization in time. In this work, the

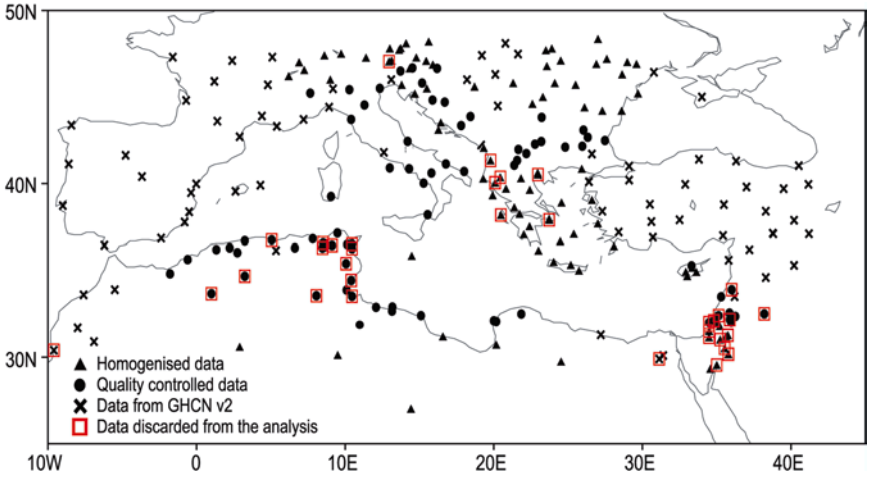

Fig. 1 Location of stations with continuous monthly records of air temperature for the period 1950–1999. The stations are separated into homogenized (*triangles*), quality controlled (*solid circles*) and GHCNv2b (*crosses*) time series. *Open squares* indicate the discarded stations from the analysis in the final CCA (see text in Sect. 3 for details)

canonical series are normalized to unit variance and the canonical correlation vectors (patterns) represent typical anomalies in the units of the variable respect to its mean state. The correlation between the canonical series measures the degree of association between the canonical patterns of predictor and predictand variables. Before CCA, the original data are usually projected onto their EOFs retaining only a limited number of them, accounting for most of the total variance and avoiding noise.

The advantages of using data in EOF space can be summarized as the independence of the data (orthogonal functions), the possibility to retain a certain number of EOFs for the subsequent CCA and the reduction of the problem's dimensionality. Discarding too many EOFs could lead us to exclude part of the significant signal and consequently to a poorer prediction of the overall CCA model. On the other hand, retaining too many EOFs could lead to an overfit of the statistical models to the particular data sets and period considered, most likely missing an adequate description of the underlying process.

During the model calibration step, the criterion was to select the number of eigenvectors for each predictor and predictand variable, which provided the best results in the cross validation process. The selected PCs are used as input for the CCA analysis and the resulting canonical patterns are regressed with the original datasets to produce the canonical components. The predictor and predictand canonical patterns are used in the verification period to estimate the regional summer temperatures from the large-scale variables in a similar manner to Zorita and von Storch (1999), González-Rouco et al. (2000, 2001) and Xoplaki et al. (2002). No lead or lag relationships were taken into consideration for this work, our analysis was restricted to simultaneous connections between the different fields and summer air temperature.

Similar CCA experiments as in Xoplaki et al. (2002) were performed though for the entire Mediterranean in two different ways: (1) nine CCA experiments relating each single predictor data (SLP, geopotential height, thickness and SST predictor fields) to summer air temperature and (2) CCA experiments (see later) with multicomponent predictors.

The first approach allows us to study the relationship between each large-scale variable and Mediterranean temperature. The second approach has the advantage of relating summer air temperatures to the joint information from various atmospheric and SST fields allowing assessment of the improvement in predictability when several predictors are used simultaneously. In this case, in order to reduce the dimensionality of the problem, two EOF analyses were applied to the predictor fields. The first one was used in order to select a few of the first PCs of each of the original variables. The resulting components were merged together and a second EOF analysis was performed on them to pick up the main modes of variation common to all predictor fields as in Xoplaki et al. (2002). Finally, a number of the resulting predictor PCs was selected to perform the CCA in combination with the PCs of the predictand field.

Detailed discussion on the EOF and CCA methods can be found in Barnett and Preisendorfer (1987), Wilks (1995), von Storch and Zwiers (1999), Livezey and Smith (1999a,b) and Smith and Livezey (1999).

3.1 The cross-validated CCA

Cross-validation is a statistical procedure used to reduce the problem of artificial skill produced by the overfitting of random variability in small samples of data (Barnett and Preisendorfer 1987; Michaelsen 1987; von Storch and Zwiers 1999). The procedure is nonparametric and can be applied to any automated model building technique. Cross-validation is a resampling technique, where the available data are repeatedly divided into validation and verification data subsets. In the model building procedure, a few observations are omitted and then the model is tested on the skipped observations. If n is the time length of the available data sets, cross-validation is carried out using calibration subsets of length m and verification subsets of length $n–m$, the number of partitions being then $n!/(m!)(n–m)!$ (Wilks 1995).

The cross-validation was applied by discarding four observations (months) from the data set in each step and then predicting them, based on the remaining data. This process was repeated for each summer season in the 50-year record. The model is fitted to the retained data (196 summer months) and used to make specification of the withheld data (von Storch and Zwiers 1999).

The performance of the statistical model was evaluated by calculating the correlation (ρ) and the Brier skill score (β, Brier 1950; Wilks 1995; von Storch and Zwiers 1999) between the predicted and the raw data. The correlation provides a measure of time concordance in the series, while the Brier score allows for a measure of the explained variance by the model (Livezey 1995). The Brier skill score is a widely used accuracy gage of quality of probability forecast accuracy, usually in relation to climatology. It is conventionally described as the relative probability score compared with the probability score of a reference forecast. It is defined as $\beta = 1 - \left[S_{FP}^2/S_P^2\right]$ where ${S_{FP}}^2$ represents the variance of the error of the forecasts F to the reference predictands P and ${S_P}^2$ stands for the variance of the predictand variable. The last term is the ratio of the error variance and the observations variance. Thus, the Brier skill score with climatology as the reference is also the proportion of explained variance. Thus, for predictions with errors which variance ranges on the order of the variance of the predictand, β will be close to 0 or negative and for predictions with a small amount of error, β tends to 1 (von Storch and Zwiers 1999). Negative predictions would indicate that climatology may be a better forecast than that tested.

For the calculation of the CCA experiments, a varying number of EOFs and canonical components were selected for the predictor and predictand variables. The objective criterion used to retain the optimal number of patterns was to select the EOFs and CCAs that provided the best results in terms of ρ and β during the validation process.

In order to improve the coherence between the predictor and predictand fields as well as accounting for a maximum amount of variance of regional air temperature, we performed a screening and excluded insignificant stations. The stations with non-significant correlation at the 99% level ($r >= 0.18$ with $n = 200$; serial correlation not included) between the cross-validated and the raw data in at least six out of the nine predictor fields were omitted. The CCA experiments have been re-performed with the reduced air temperature (213) time series. The discarded air temperature stations are indicated by open squares in Fig. 1.

As a first step before the EOF and CCA analyses, the annual cycle was removed from all station and grid point time series by subtracting from each monthly value the respective month's 1950–1999 long-term mean. In order to account for the latitudinal distortions, each grid point of the large-scale field anomalies was weighted by the square root of cosine of latitude (φ) to ensure that equal areas are afforded equal weight in the analysis (North et al. 1982). The long-term stationarity of the time series is preserved for the calculation of EOF and CCA through detrending the time series with a linear least square fit. Subsequently, eigenvectors (canonical vectors) are obtained via diagonalization of the covariance (cross-correlation) matrix. Once the eigenvectors (canonical vectors) are available, the PCs (canonical series) can be obtained through regression (von Storch and Zwiers 1999) of the original not detrended dataset with the eigenvectors (canonical vectors).

4 Results

Figure 2 presents the spatial and temporal characteristics of summer (JJAS) temperature over the Mediterranean between 1950 and 1999. For the purpose of comparison, observational data are plotted with NCEP reanalysis values (Kalnay et al. 1996; Kistler et al. 2001). Figure 2a, b shows the average and standard deviation patterns at the 213 sites (colour shading) and in the

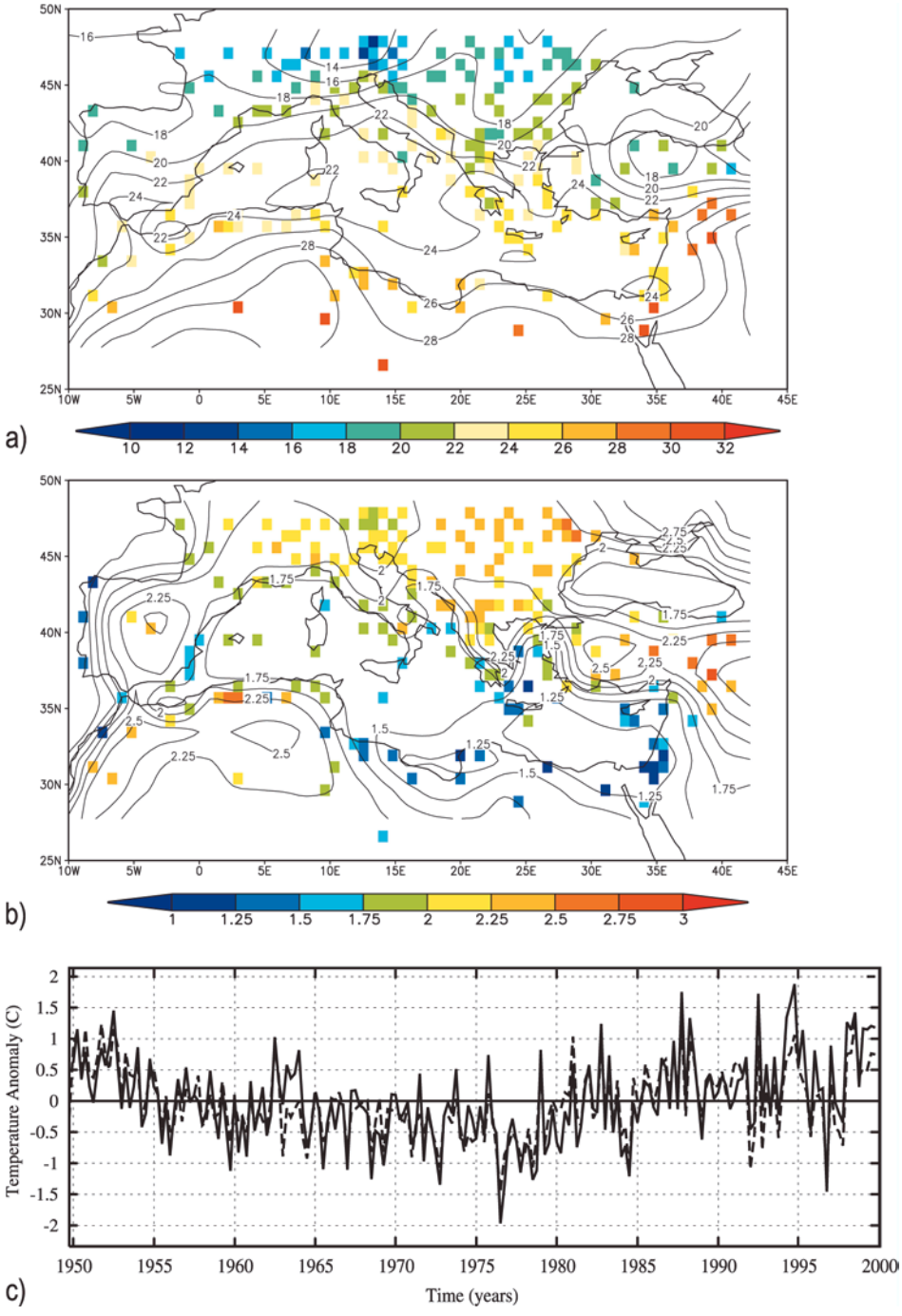

Fig. 2a–c Spatial and temporal characteristics of the Mediterranean summer (JJAS) temperature; 1950–1999. **a** Summer mean temperature over the 213 Mediterranean sites (*grey shading*) and from the NCEP-reanalysis data (*contours*). **b** Summer temperature standard deviation over the Mediterranean stations (*grey shades*) and based on the reanalysis data (*contours*). **c** Mediterranean monthly summer temperature anomalies (land areas) for the observations (*solid line*) and the reanalysis data (*dashed line*)

reanalysis data (contours). The most extensive areas of summer high air temperatures up to 30–32 °C are over the desert areas of North Africa and the Near East. At the northernmost part of the area under consideration, the summer temperatures are approximately 10 °C lower. Standard deviations reveal the opposite with increasing variability from south to north, ranging from values of 1 °C in the southeast to 3 °C in the northern areas. In general, there is good agreement in the behaviour of the observations and reanalysis data. Local discrepancies arise due to the higher resolution of the observations that present more spatial variability. In this first approach, picturing the variability of the data, land–sea contrast appears as the main factor controlling the mean and deviation of temperature over the region under investigation. The sharp gradients in the standard deviation along the coastal areas are obvious in Fig. 2b pointing to the thermal moderating effect of the ocean.

Figure 2c depicts the monthly time evolution of the summer temperature anomalies (land areas) over the region, both for the observations (solid line) and the reanalysis data (dashed line). The coolest periods in the Mediterranean were the 1960s and 1970s, with the coolest year in 1976 and the warmest summers in 1994

and 1999. Therefore, decadal variability during this period reveals cooling in the 1950s and warming since the mid 1970s. The trend for the period 1950–1960 is –1.15 °C/decade and 0.5 °C/decade for the period 1980 to 1999 (both trends evaluated on the observational data and are significant at the 95% level, allowing for autocorrelation). The trend over the entire 50 years from 1950–1999 is 0.08 °C/decade (statistically significant at the 95% level, allowing for autocorrelation). Here too, a good agreement between observations and reanalysis is found, pointing to a good quality in both datasets and the robustness of the trends described.

4.1 CCA in EOF space

The different EOF–CCA-cross-validation experiments for the Mediterranean summer air temperature are summarized in Table 1. In the first column, the different predictors (geopotential heights, SLP, thickness fields and SSTs) are presented. The second column shows the number of predictor and predictand EOFs retained for each experiment either unicomponent or multicomponent. The cumulative explained variance of the predictor fields is given in the fourth column. In columns five to eleven, a summary of the EOF-CCA experiments is shown. Columns five to seven contain the canonical correlations (r_1, r_2 and r_3) of the first three CCA pairs between the circulation, thermal predictors and the summer air temperature, while the corresponding explained variance (TT-Exp. Var. 1) for the predictands is given in the following three columns (columns eight to ten). The eleventh column reveals the total explained variance (TT-Tot. Exp. Var. 1–3), taking into consideration only the first three canonical pairs. The last two columns present the performance of the models; in the second last column, the performance is presented in terms of the correlation skill score (ρ) whereas the last column shows the Brier skill score (β), as described in the methods section. The ρ and β values presented in Table 1 correspond to the spatial average over all the ρ_i and β_i ($i = 1, \ldots, 213$).

The connection between each single large-scale predictor field and the summer air temperature has been investigated, and its results are shown in rows two to nine of Table 1. The second approach deals with the combined influence of three predictors and its results for summer air temperature are presented in rows 11 and 12.

4.1.1 Unicomponent EOF–CCA-cross-validation

For the Mediterranean summer air temperature the EOF–CCA-cross-validation experiments with single predictor fields were conducted with the leading eight predictor data EOFs, accounting for between 64.6% (700–1000 hPa thickness) and 91.2% (SSTs) of the total variance (Table 1) and the three and five leading air temperature EOFs, explaining 66.2% and 75.7% of the

Table 1 Summary of CCA results. Columns 1 to 3: predictor variable(s), number of predictor(s) and predictand EOFs. Column 4: percentage of accumulated EOFs variance. Columns 5, 6 and 7: canonical correlations for the first three CCA modes. Columns 8, 9 and 10: variance, each canonical mode accounts for, in the predictand (Mediterranean temperature). Column 11: total explained variance by the three modes. Columns 12 and 13: correlations and Brier score from the cross-validation

Predictor	X-EOFs	Y-EOFs	X-Cum. Var. (%)	CCA r_1	CCA r_2	CCA r_3	TT-Exp. Var. 1 (%)	TT-Exp. Var. 2 (%)	TT-Exp. Var. 3 (%)	TT-Tot. Exp. Var. 1–3 (%)	ρFP	B_{FRP}
300 hPa	8	5	77.4	0.84	0.75	0.66	24.2	22.2	13.1	35.3	0.48	0.22
500 hPa	8	5	79.2	0.83	0.75	0.63	24.3	18.3	15.6	33.2	0.44	0.18
700 hPa	8	5	80.0	0.83	0.73	0.59	22.7	16.6	17.4	30.5	0.40	0.14
850 hPa	8	5	80.7	0.80	0.70	0.55	19.8	15.0	18.4	25.6	0.38	0.14
SLP	8	5	78.7	0.76	0.68	0.53	15.0	13.5	24.5	21.8	0.36	0.12
300–500 hPa	8	5	69.8	0.78	0.71	0.64	22.5	19.1	13.9	29.0	0.43	0.17
500–700 hPa	8	5	68.4	0.83	0.73	0.68	18.7	36.8	7.0	35.7	0.48	0.22
700–1000 hPa	8	5	64.6	0.92	0.90	0.75	22.5	36.2	6.1	51.8	0.62	0.39
SST	8	5	91.2	0.89	0.76	0.65	25.3	24.0	9.1	37.7	0.60	0.36
All fields 90%	16	5	–	0.94	0.86	0.86	31.7	26.0	7.6	53.2	0.66	0.45
3 fields 80%	16	5	–	0.97	0.94	0.91	30.6	23.9	7.7	56.3	0.75	0.58

summer variability, respectively. The results contained in Table 1 refer to five retained summer air temperature EOFs, with significantly better model performance than three EOFs.

According to the total explained variance of the Mediterranean summer air temperature, the most skilful circulation predictors are the 300 hPa and 500 hPa geopotential heights. The best thermic predictor is the 700–1000 hPa thickness field followed by the Mediterranean SSTs. Atmospheric thickness and SSTs tend to perform better than circulation predictors do. Poorer performance is obtained using the SLP as predictor variable. Cross-validation (last two columns of Table 1) mostly confirms the behaviour of CCA1, with higher (lower) skill on the upper levels concerning the geopotential (thickness) fields.

4.1.2 Multicomponent CCA

Several CCA experiments with multicomponent predictor fields and temperature have been designed (Table 1). In the first EOF analysis of each predictor field, tests were made selecting 80%, 85% and 90% of variance. In addition, several experiments have been performed with varying numbers of retained EOFs prior to the CCA. The best performance was obtained by selecting 80% of variance from each predictor field and retaining 16 PCs in the second EOF analysis of the predictor variables. For the summer temperature predictand variable, a number of five PCs (77.5% variance) was retained before performing the CCA.

The calculations with the Mediterranean summer air temperature as predictand were applied with various numbers of EOFs for the large-scale and for the predictand fields. Several experiments have been conducted with the full set of the nine large-scale predictors. Compared to the unicomponent experiments, no significant gain has been obtained either in the total explained variance or in the model's performance (Table 1, row 11). For this reason, we performed another experiment only with the three large-scale fields, explaining the highest amount of variability and with best performance in the cross-validation procedure in the unicomponent cases. Thus, the 300 hPa geopotential heights field, the 700–1000 hPa thickness and the Mediterranean SSTs have been selected as predictors, with considerable improvement of the model (Table 1, row 12). Considerably higher values in the total explained variance of the Mediterranean summer air temperature are achieved by applying the multicomponent CCA experiments. Moderate gain is obtained in the performance of the model (last two columns in Table 1). More than 50% of the Mediterranean summer air temperature is explained by the three combined predictors.

The results of the multicomponent CCA experiments including three predictor fields for summer temperature are described in the following section with the aim of studying the interannual covariability between the Mediterranean summer air temperature and the combined large-scale circulation at different levels, thickness and SST fields during the period 1950–1999.

4.2 Maps of CCA results

The relationship between the interannual variability in the three large-scale predictors with best performance in the unicomponent CCA (300 hPa geopotential heights, 700–1000 hPa thickness and Mediterranean SSTs) and Mediterranean summer air temperatures is studied by means of multiple CCA in the EOF space. Canonical series and their associated spatial vectors for the leading two modes are presented in Figs. 3 to 6. All the maps in these figures are regression maps between the resulting canonical series and the original fields, thus, anomalies indicate realistic deviations in the physical units of each variable. These figures can be interpreted with the present sign configuration or with opposite sign both for the patterns and the time series.

Figure 3 presents the results for the first canonical mode using three large-scale predictors for local summer air temperature over the larger Mediterranean area. In the case of the three predictors 16 EOFs were retained; for the Mediterranean summer air temperature five EOFs were selected (see Table 1). The first CCA exhibits a correlation between the multicomponent 300 hPa geopotential height, 700–1000 hPa thickness, Mediterranean SST fields and the summer air temperature of 0.97. CCA1 accounts for 30.6% of the summer temperature variability. The canonical component (Fig. 3) of the 300 hPa geopotential height field explains around 4% of the total upper height variability. The spatial pattern shows strong positive anomalies centred over Central Europe. A region of negative anomalies with its centre over southeast Greenland extends to the north–east around the area of positive anomalies. The western and central Mediterranean is dominated by this large-scale anomaly whereas the eastern Mediterranean is only marginally influenced.

The 700–1000 hPa thickness pattern indicates a similar structure as the 300 hPa geopotential height field, with a warm troposphere over much part of Europe and the central and western Mediterranean. From Libya to Turkey and the entire Near East, there is evidence of a cooler lower troposphere. The pattern accounts for around 5% of the total large-scale summer thickness variability.

The SST anomaly pattern reveals a monopole pattern with positive (negative) values over the entire basin. Maximum departures are prevalent in the Ligurian Sea (northern Italy and southern France), the lowest values are found in the western basin and the Levant Sea. This pattern accounts for around 28% of summer Mediterranean SST variability.

The summer surface air temperature pattern exhibits a gradual decrease of positive anomalies from Central Europe towards the eastern Mediterranean. Egypt and the Near East countries indicate slightly negative

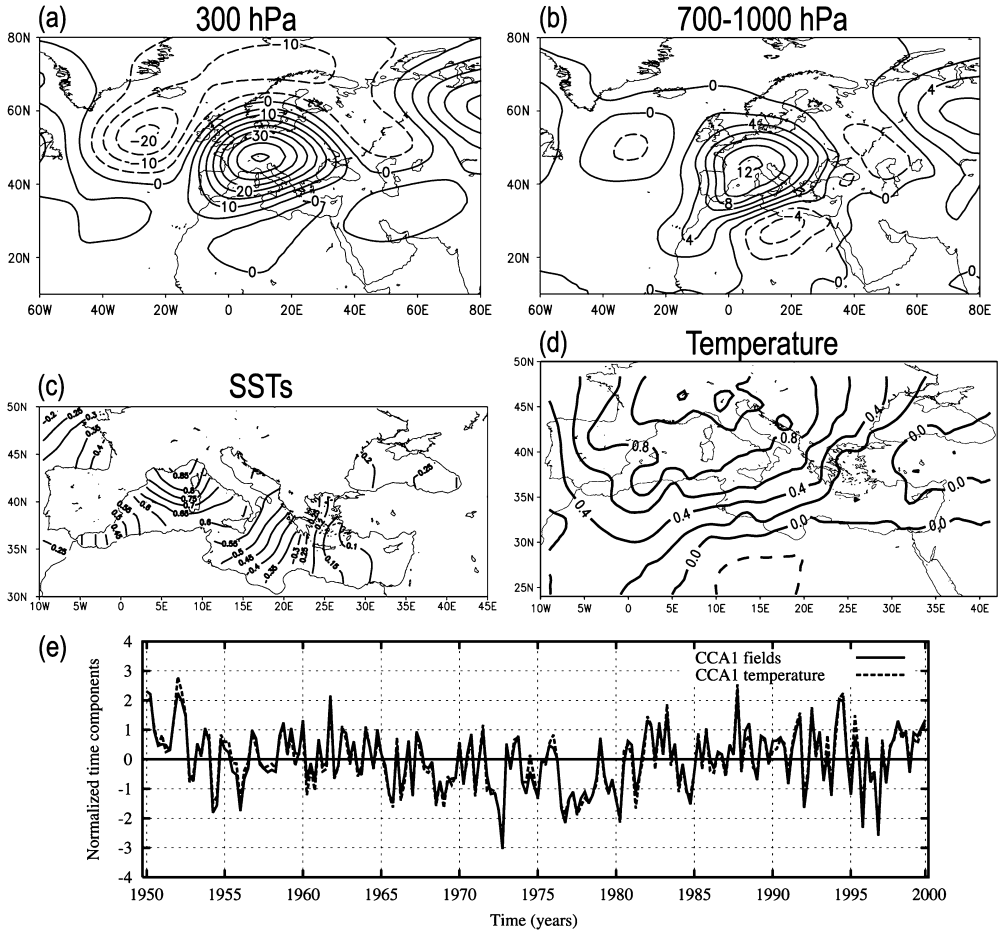

Fig. 3 Canonical spatial patterns of the first CCA. The canonical correlation patterns reflect the typical strength of the signal, with **a** 300 hPa. **b** 700–1000 hPa. **c** SST. **d** air temperature anomalies in °C. **e** normalised time components of CCA 1

temperature anomalies. This anomaly configuration seems to follow that of the 700–1000 hPa thickness field.

Figure 3e shows the first pair of canonical series indicating variability from monthly to interdecadal scales. The late 1960s and 1970s present a tendency to more frequent negative values of the canonical series suggesting a higher frequency of states in which the patterns described appear with the reversed sign. The 1950s and 1990s indicate however a tendency to positive values. This forms the interdecadal variability in this canonical mode showing a negative trend since the beginning of the period to the late 1970s and a positive trend since then to the end of the twentieth century. The correlation between this series and the spatial average of summer temperature in Fig. 2c is 0.76 (significant at the 95% level). Thus, it seems that there is an important contribution from this canonical mode to the long-term trends in regional temperature over the Mediterranean. This topic will be further addressed in the discussion section.

Figure 4 shows complementary information presenting the regression maps between the first canonical series and several geopotential height variables (500 hPa, 700 hPa, 850 hPa), thickness fields (300–500 hPa, 500–700 hPa), SLP and surface temperature as provided by the NCEP reanalysis (Kalnay et al. 1996; Kistler et al. 2001). SLP and the geopotential height variables show virtually the same large-scale structure as the 300 hPa field. The amplitude of the anomalies in the geopotential height variables seems to increase with height. Thickness fields are also comparable to the 700–1000 hPa anomalies shown in Fig. 3b. Figure 4g reveals a remarkable agreement with Fig. 3d indicating that the temperature anomalies described above extend further northward to the British Isles and southern Scandinavia.

The second CCA mode (Fig. 5) (0.94 correlation) explains around 6% of the 300 hPa and 700–1000 hPa predictors, 16% of the SSTs variance and 24% of the Mediterranean summer air temperature. The pattern of the 300 hPa geopotential height indicates a negative anomaly centred over the North Sea region covering the northwestern part of the larger Mediterranean area; an area of positive anomalies extends from the Ural mountains to the south and west reaching the eastern half of the Mediterranean. The pattern of the 700–1000 hPa anomaly fields resembles that of the 300 hPa geopotential height field showing a colder (warmer) area in the western part of the Mediterranean under the negative (positive) geopotential height anomaly.

The east–west structure appears also in the SST anomaly field with positive (negative) values east (west) of around 10°E including the Black Sea. However, the differences in °C are rather small.

Negative summer air temperature anomalies over Switzerland, France, Spain and Portugal can be related

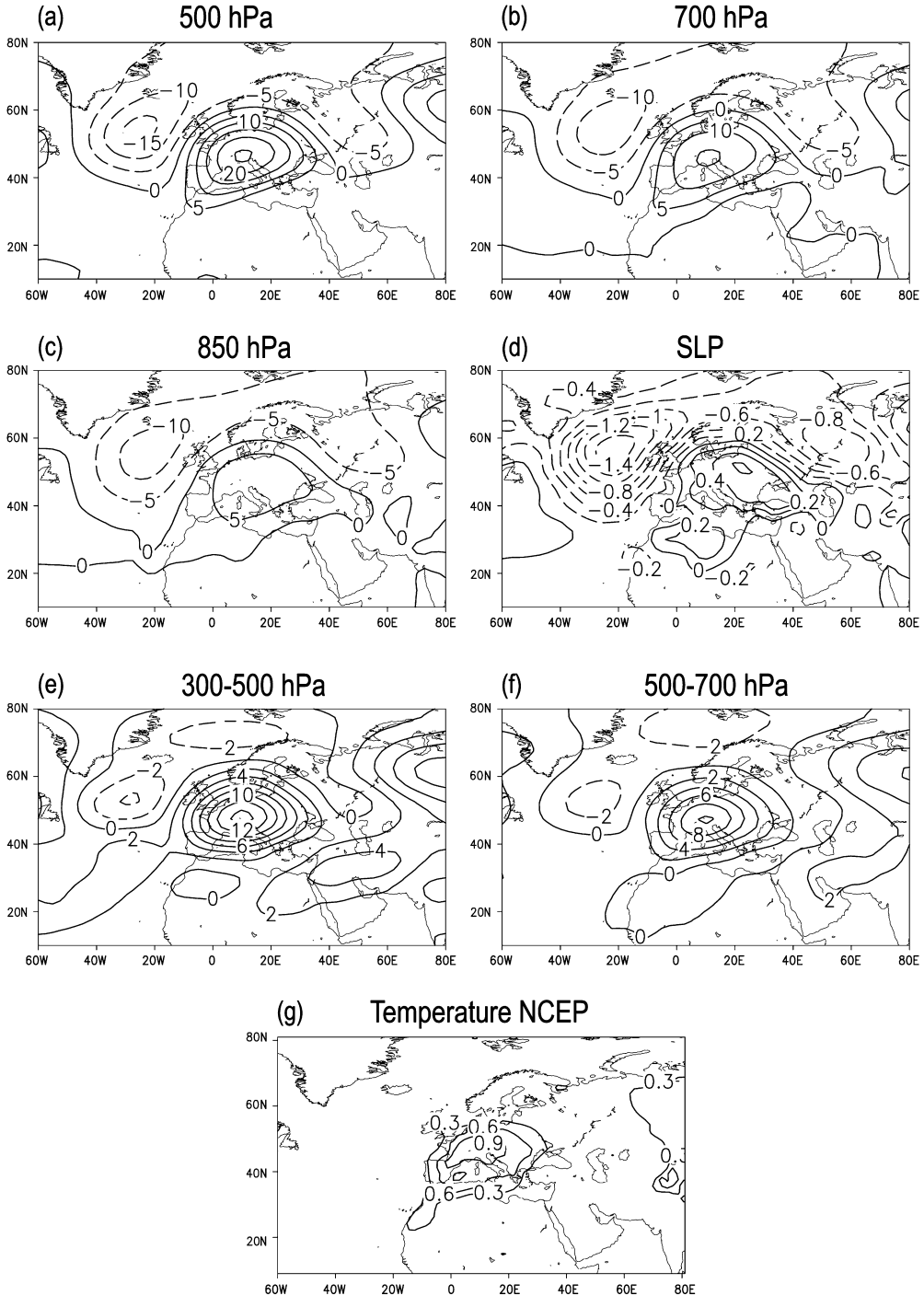

Fig. 4a–g Regression maps between NCEP large-scale variables and the Mediterranean temperature first canonical series shown in Fig. 3e

to the influence of the large-scale negative upper level anomaly, a cooler lower troposphere and lower SSTs over the western Mediterranean. Over the majority of the larger Mediterranean area, warmer summer conditions are connected with an upper level ridge, a warming within the first 3500 m and positive SSTs.

The second pair of canonical series (Fig. 5e) shows intense negative anomalies in the summers of 1976, 1983 and 1989, and positive in 1952 and 1999. In general, it is apparent that there was a negative phase from the late 1960s to the end of the 1970s and positive phases in the 1950s and 1990s. Thus, as in the case of the first canonical series there seems to be a contribution on decadal and long-term variability from this canonical mode. The correlation between this series and the spatial average of temperature in Fig. 2c is 0.58 (significant at the 95% level).

Figure 6 shows regression maps between the second temperature canonical series and the large-scale variables that were not used as predictors in this analysis, as well as surface temperature from the NCEP reanalysis. Once again, the geopotential and thickness

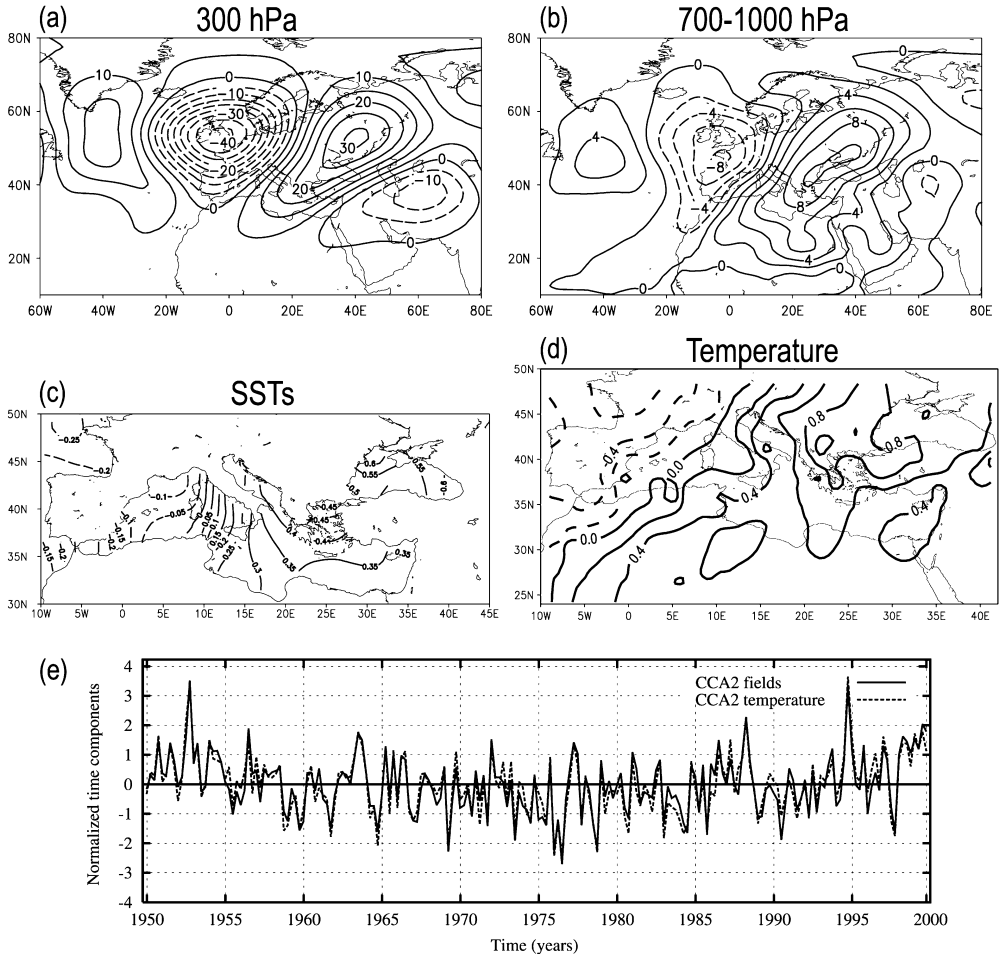

Fig. 5 Canonical spatial patterns of the second CCA. The canonical correlation patterns reflect the typical strength of the signal, with **a** 300 hPa. **b** 700–1000 hPa. **c** SST. **d** air temperature anomalies in °C. **e** normalised time components of CCA 2

variables follow the configurations already described for the second CCA mode. The analysis highlights stronger geopotential anomalies on the highest levels. For instance, it can be pointed out that the signature of the region of positive anomalies over Russia vanishes almost completely for the lower troposphere. This feature will be considered in more detail in the discussion section.

The surface temperature (NCEP) regression map, though with lower resolution than that of Fig. 3e, provides a broader spatial perspective. It shows that positive and negative anomalies in the Mediterranean area extend northward mimicking the areas covered in extension by the negative and positive anomalies in the upper geopotential height and thickness variables.

Figure 7 shows the spatial distribution of skill using the model with three predictors (300 hPa geopotential height, 700–1000 hPa thickness and SSTs) as presented in Figs. 3 to 6. Essentially, both the correlation and the Brier skill score indicate a very similar spatial structure with higher values in the northern half of the studied area. Therefore, in these regions the downscaling model performs better. We should bear in mind that this is the region with higher variance in the dataset (Fig. 2b). It should also be pointed out that this skill pattern is somewhat reminiscent of the first canonical vector of Mediterranean temperature (Fig. 3d), a reasonable finding considering that this is the mode that accounts for more regional variance. This behaviour in the skill was also found in the downscaling approach of González-Rouco et al. (2000) for precipitation in the Iberian Peninsula.

5 Discussion

The description of the mean state and the variability of recent climate has implications in several aspects of regional climate change research: monitoring and detecting climate change, calibration of or merging with satellite data, climate model evaluation, biogeochemical modelling, and construction of climate change scenarios (New et al. 1999).

As stated in the introduction, progress in understanding climate variability in the Mediterranean area is not only an issue of interest in itself, but also of relevance for society and natural ecosystems (IPCC 2001). Climatic extremes predictions and potential changes expected from an increase in anthropogenic emissions depend on the knowledge of the meaningful modes of large-scale climate which drive regional climate changes and extremes.

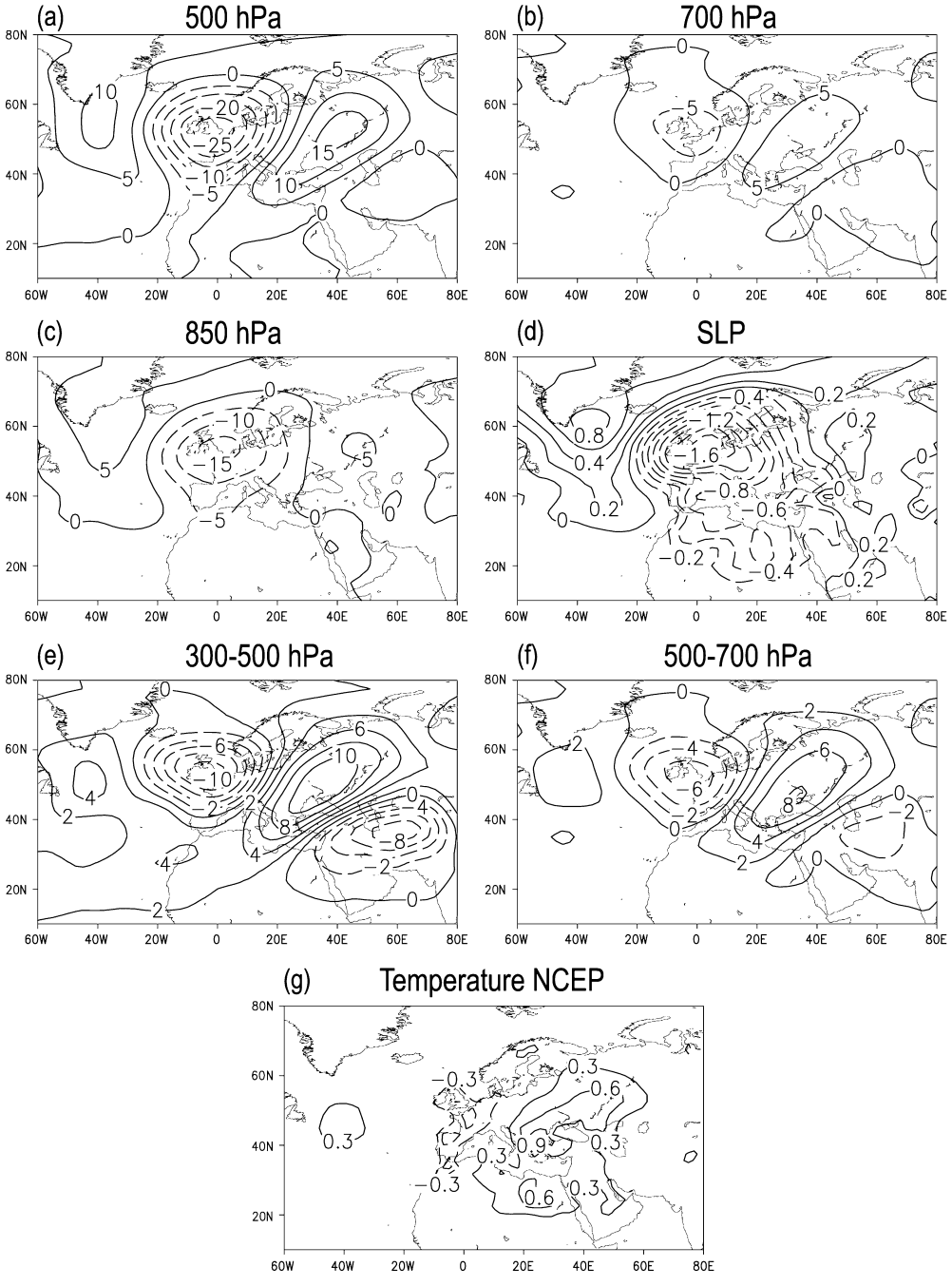

Fig. 6a–g Regression maps between NCEP large-scale variables and the Mediterranean temperature second canonical series shown in Fig. 5e

This work tries to contribute to the understanding of climate variability in the Mediterranean area. The results presented in the last section show that about 56% of the summer Mediterranean temperature variability during the second half of the twentieth century can be explained by making use of three canonical modes.

The large-scale patterns for the first CCA mode (Figs. 3, 4) reveal a dipole configuration in the North Atlantic. In the positive phase of the dipole a deep centre with positive 300 hPa geopotential height anomalies is located over Central Europe; an area of negative anomalies presents higher values south of Iceland and the surrounding northern region; the positive anomalies extend to the western Ural mountains and the northern Caspian Sea. As described in the last section the other geopotential variables and thickness fields show a similar configuration indicating higher (lower) temperatures in the high (low) pressure regions. SSTs and surface temperatures reveal higher values in the northwestern part of the Mediterranean under the high pressure region.

This dynamic configuration strengthens the zonal flow over Northern Europe and the easterly–northeasterly flow over the Mediterranean. The increased stability leads to clear sky conditions and maximum insolation in the area. Xoplaki et al. (2002) have shown that

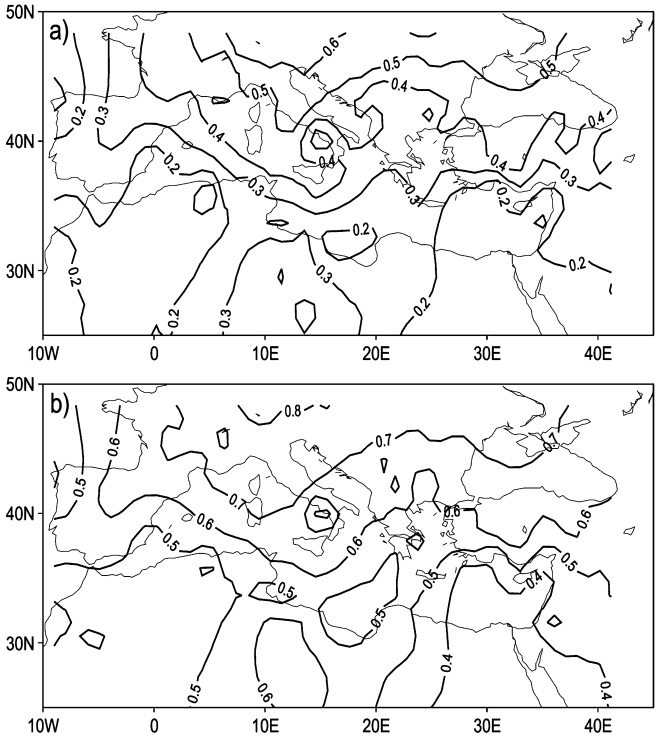

Fig. 7 **a** Spatial distribution of correlation **b** Brier skill score obtained from cross-validation for the model with three large-scale predictors

precipitation presents positive correlation values with the negative geopotential height regions and negative values with the positive geopotential height areas supporting the presence of clear skies and stability in the warm highs. Thus, the radiative 'bonus' favoured by the dynamical configuration could be the main factor allowing for the higher temperatures in the warm high pressure regions. The SSTs anomaly structure follows that of the atmospheric anomalies. Since the atmospheric structure dominates over a much larger area than the sea anomaly pattern and also over the whole troposphere, we suggest that the atmosphere seems to be the forcing agent for the ocean in this CCA mode.

The negative phase of the first CCA mode can be discussed reversing the sign in the previous reasoning. If the positive phase can be made responsible for a reinforcement of the zonal flow over Northern Europe, the negative phase would contribute to a weakening of it, allowing for winds with westward components over the Baltic Sea and strengthening of the westerlies and southwesterly flow in the Mediterranean. As described by Xoplaki et al. (2002), this behaviour could be labelled as that of a 'high-index' type: for the positive (negative) phase of this CCA mode, negative (positive) anomalies dominate in higher latitudes and positive (negative) ones over the Mediterranean. This leads to a weakened (intensified) zonal flow to the Mediterranean and northward (southward) shift of the Subtropical Jet (300 hPa).

Concerning the second CCA mode (Figs. 5, 6), the 300 hPa field shows a configuration of zonally distributed anomalies of alternating sign and extending from southern Greenland to the Middle East. A similar reasoning can be made as in CCA1 about the warm highs (cold lows) favouring (inhibiting) radiative warming. From the dynamical point of view, the circulation configuration can be pictured, as in Xoplaki et al. (2002) as that of a 'low-index' type. In summer months with high positive values of this CCA mode there is an increase in the frequency of anomalous meridional flow over Europe, from Scandinavia towards the western Mediterranean, connected with the Polar Front Jet meandering between a low centred over Great Britain, a high over Eastern Europe and a low to the southeast of the Caspian Sea. The negative phase of the mode reveals the opposite sign configuration. In this context, SSTs and surface temperatures behave in accordance with the atmospheric patterns, with negative anomalies below the cold low (western Mediterranean) and positive anomalies under the warm high (central and eastern Mediterranean). As in the previous mode, the SSTs seem to follow the atmospheric anomalies under the surplus (highs) or deficits (lows) of radiation. At the surface, the SLP pattern shows some signs of the high pressure system over Russia, but over the Mediterranean it has completely given way to the low pressure system over Great Britain which extends to the southeastern borders of the Mediterranean. This configuration favours winds from North Africa and the Sahara to the central and western Mediterranean area, contributing to the warmth in these areas (Maheras and Kutiel 1999).

The first CCA mode described in this section agrees well with the second mode in the study of Xoplaki et al. (2002) on summer temperatures over Greece, whereas the second mode of influence for Mediterranean temperatures coincides well with the first mode. Thus, it seems plausible to extend the reasoning in their work to the entire Mediterranean area. From this perspective, the variability of summer temperatures in the Mediterranean would be well described with a parsimonious conceptual model invoking two modes, the 'high-index' type and the 'low-index' type, which picture transitions from the zonal to the meridional flow.

The canonical series corresponding to both CCA modes shown in Figs. 3e and 5e correlate well with the spatial average of Mediterranean summer temperature: 0.76 and 0.58 for the first and second canonical mode, respectively. Actually, direct contributions to some specific exceptional temperature episodes can be directly determined from observation of Figs. 2c, 3e and 5e. For instance, the high temperatures in the 1994 and 1999 Mediterranean summers correspond well with peak values in the scores of both canonical series. The first canonical mode seems to have contributed to the high scores in the early 1950s and the negative ones in 1996 while the second mode played an important role in the exceptional 1964 summer that was warm for the central and eastern Mediterranean and cooler for the western regions. It is also worth mentioning the summer of 1976, which was the coolest in the second half of the twentieth

century (Fig. 2c) and can be attributed to the lowest scores in the second canonical series (Fig. 5e). According to this analysis, the second canonical mode presented its negative phase in 1976, with a deep low affecting the central and western Mediterranean (Xoplaki et al. 2002) and a high centred over the British Isles reaching the western borders of the Mediterranean. Thus, this accounts also for the very warm conditions experienced in Great Britain (Ratcliffe 1978) at that time.

Concerning long-term trends, it seems that both canonical series have contributed to the cooling trend in the 1960s and the warming trend in the1980s. This is a difference to Xoplaki et al. (2002) where no contribution to long-term trends is found on the 'high-index' mode. A possible explanation for this is that their analysis is restricted to a part of the eastern Mediterranean. In this area the first canonical component shown herein (second component in their analysis) is less intense, a feature that could have made trends less evident in their analysis.

Figure 8 allows for a further remark concerning long-term trends and the associated large-scale configurations. The use of SLP data from the NCAR dataset (Jenne 1975; Trenberth and Paolino 1980) allows for a broader perspective on trends since the beginning of the twentieth century. The time series labelled CCA1 and CCA2 in Fig. 8 show the regressed time series (10-years moving average filter outputs) between the SLP dataset (1900 to 1999) and the SLP patterns in Figs. 4d and 6d, respectively. Previous to this step, the regression patterns were interpolated to the same spatial resolution (5°×5°latitude × longitude) as the SLP dataset. These time series can be considered as an estimation with minimum error of the intensities of the canonical series in Figs. 3e and 5e through the entire twentieth century using the information provided by the SLP dataset. In Fig. 8, CCA1 and CCA2, show distinct cooling trends in the 1960s and 1980s, in agreement with these statements. However, their behaviour for the first half of the century is rather different: while CCA2 indicates a clear decreasing trend through the whole period, CCA1 shows high values in the 1920s and 1950s and a deep minimum around 1910. The solid line in Fig. 8 (labelled Spatial average) presents the standardized time series (10-years moving average filter output) of the spatial average of Mediterranean temperature using the dataset presented in Fig. 1. CCA1 and the Mediterranean temperature show a remarkable agreement in their evolution throughout the twentieth century. The correlation between the spatial average time series and CCA1 and CCA2 is 0.86 (significant at the 95% level, allowing for fewer degrees of freedom due to the filter) and –0.1 (not significant), respectively. A CCA was made using the NCAR SLP dataset as a single predictor and Mediterranean temperatures (62 stations) for the period 1900 to 1999 (not shown here). The same time evolution as shown in Fig. 8 was found.

Therefore, in view of these results we suggest that the long-term trends in Mediterranean summer temperatures through the twentieth century are inherently related to the variation of the first canonical mode ('high-index' type) described before. The associated patterns between the surface of the atmosphere (SLP) and the upper atmosphere variables (geopotential and thickness variables) described by the first canonical mode in Figs. 3 and 4 can be assumed to remain stable in time. Thus, it can be argued that during the first half of the twentieth century, the upper levels of the atmosphere should have behaved in accordance to the CCA1 time series in Fig. 8.

The spatial average for Mediterranean temperatures also describes the evolution of temperatures during the second half of the twentieth century showing high values during the 1860s (13 stations), comparable to those during the 1950s and 1990s. For the period 1850 to 1999, a trend of 0.018 °C/decade is found (significant at the 95% level). For the period 1900 to 1999, a change of 0.05 °C/decade is found. This points to an increase in temperature of about 0.27 °C in the 1850–1999 period, and of 0.5 °C in the twentieth century. This result agrees in its order of magnitude with the warming trend indicated by Folland et al. (2001) though their infra-estimates show 0.75 °C as the warming value for the whole century. The reasons for this difference could also be in the different datasets used.

The modes of concurrent CCA pairs between Mediterranean temperature and the large-scale 500 hPa fields presented by Corte-Real et al. (1995) also indicate the presence of a four centred pattern causing higher than

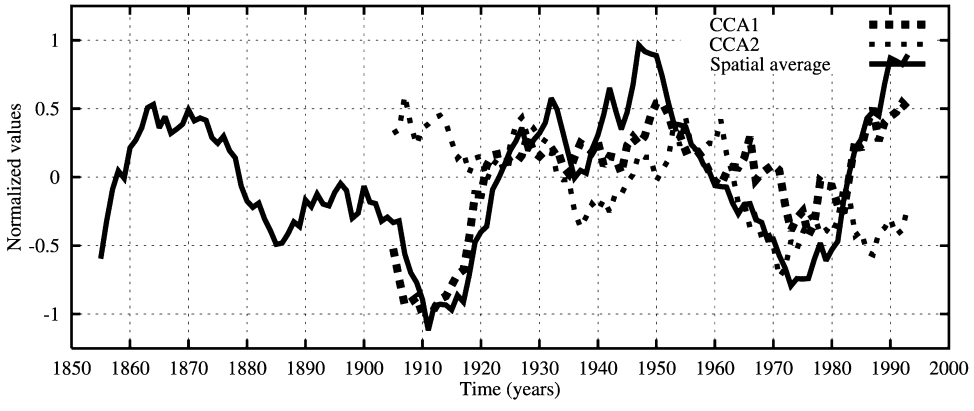

Fig. 8 Regressed time series (*dashed lines*) between the SLP NCAR (Trenberth and Paolino 1980) dataset and the SLP patterns in Fig. 4d (CCA1) and Fig. 6d (CCA2). The *solid line* (spatial average) corresponds to standardized values of the spatial average of Mediterranean summer temperatures for the period 1850 to 1999. All time series are outputs of a 10-years centred moving average filter

normal temperatures to the central and eastern Mediterranean. The location and intensity of the leading anomaly patterns within the two first CCAs revealed some differences.

Corte-Real et al. (1995) investigated the connections between the non-seasonal connection between regional climate and the large-scale atmospheric circulation at the 500 hPa level. Thus, these results can only partly be compared with our findings due to the different temporal and spatial resolution as well as the different EOF-CCA experiments.

6 Conclusions

In this study, the interannual to decadal connection between the Mediterranean summer (JJAS) surface air temperature, as expressed by 213 station time series, and the state of the large-scale atmospheric circulation, the thickness patterns as well as the Mediterranean SSTs, was investigated for the period 1950–1999.

Warmer Mediterranean summers characterize the 1950s, 1980s and 1990s and cooler summers were prevalent from the mid-1960s to the mid-1970s. We found a significant warming of 0.05 °C/decade over the 1980 to 1999 period. For the whole twentieth century, the significant upward trend is of the order of 0.05 °C/decade.

The CCA experiments with the combined, multi-component large-scale predictors and summer temperature served to investigate the covariability between geopotential height and large-scale thermal fields and the Mediterranean summer air temperature. The combined information of the 300 hPa geopotential height field, the 700–1000 hPa thickness and the Mediterranean SSTs account for more than 50% of the Mediterranean summer temperature variability for 1950–1999. Additional predictors did not improve the statistical model.

The two canonical modes found agree well with those of Xoplaki et al. (2002) and can be expressed in a simple conceptual model invoking high-index and low-index type of circulation configurations. The first CCA mode (high-index type) pictures shifts on the zonal flow. In its positive phase it is related to warm summers, blocking conditions, subsidence and stability over the Mediterranean. Further, warm summers can be attributed to a warm lower troposphere as shown by thickness variables and positive Mediterranean SSTs. The second CCA component (low-index type) is associated with intrusions of cold air in the upper atmospheric levels that derive from a jet stream meandering between high and low geopotential height anomalies of alternating sign, which extend from the southwest of Greenland to the Caspian Sea. In its positive phase, this mode leads to a warmer (colder) central and eastern (western) Mediterranean, thus a dipole pattern over the basin.

Both modes contribute to the trends in the second half of the twentieth century, though it is shown that only the first mode is related to the long-term trends for the entire twentieth century. Thus, we suggest that the high-index type situations regulate the long-term changes in Mediterranean summer temperature allowing for a surplus (deficit) of solar radiation reaching the surface in the positive (negative) phase of the first canonical component when high (low) pressure systems are persistent in the area.

During the 1900 to 1999 period, summer Mediterranean temperature increased by 0.5 °C. Since the beginning of the records (1850), the increase in summer temperature has been found to be 0.27 °C.

Our results contribute to the understanding of climate variability in the Mediterranean area during the twentieth century. Implications can also be derived for the climate change discussion since regional changes due to the increase of the concentrations of greenhouse gases and aerosols would be partially imposed by the large-scale through changes in the intensity and frequency of the patterns described herein (first CCA mode). An appropriate assessment of the simulation of the described modes of variability by AOGCMs is needed as model validation as well as insight of the extent to which the regional to large-scale relationships are modified in scenario simulations. This type of assessment can contribute to provide scenario predictions of temperature and precipitation with high resolution using the modes of variability described in this work as a reference.

Acknowledgements The authors wish to express their thanks to the following institutions or persons, who kindly provided their valuable climate time series, through which the climate analysis for the Mediterranean region were made possible (in alphabetical order of the countries): Albania: Prof. Sanxhaku, Academy of Sciences, Hydrometeorological Institute, Tirana; Algeria: Dr. M. Kadi, Office National de la Météorologie Climate Center, Dar el Beida, Algiers Austria: Dres. I. Auer, R. Böhm and W. Schöner, Zentralanstalt für Meteorologie und Geodynamik (ZAMG), Vienna; Bosnia-Herzegovina: Dr. E. Sarac, Federal Meteorological Institute, Sarajevo; Bulgaria: National Institute of Meteorology and Hydrology, Bulgarian Academy of Sciences, Sofia and D. Lister, Climatic Research Unit, University of East Anglia, Norwich, UK; Croatia: Dr. M. Gajic-Capka, Meteorological and Hydrological Service of Croatia, Department for Meteorological Research, Zagreb; Cyprus: Dr. L. Hadjioannou, Ministry of Agriculture, Natural Resources and Environment, Meteorological Service, Nicosia; Greece: Hellenic National Meteorological Service, Hellinikon, Athens; Israel: Dr. A. Porat, Ministry of Transport, Israel Meteorological Service, Bet Dagan; Italy: Colonel Dr. M. Capaldo, Aeronautica Militare, Centro Nazionale di Meteorologia e Climatologia Aeronautica Aeroporto Pratica di Mare, Pomezia; Jordan: Dr. H. AL Sha'er, The Hashemite Kingdom of Jordan, Meteorological Department, Climate Division Amman Civil Airport, Amman; Lebanon: Dr. A. Bejjani, Republic of Lebanon, Ministry of Transport, Meteorological Services, Beirut; Libya: Dr. K. Elfadli, Libyan Meteorological Department, Climatological and Agrometeorological Section, Tripoli; Moldavia: Dr. L. Fisher, Hidrometeo Service (Chimet), Chisinau; Romania: Dr. A. Busuioc, National Institute of Meteorology and Hydrology, Bucharest; Skopje: Dr. N. Aleksovska, Hydrometeorological Institute of the FYR Macedonia, Meteorological and Climatological division, Skopje; Slovenia: Dres. T. Ovsenik-Jegliè, J. Miklavčič and B. Zupančič, Hydrometeorological Institute of Slovenia, Ministry of the environment and Physical Planning, Ljubliana; Switzerland: Swiss Meteorological Office (MeteoSchweiz), Zurich; Tunisia: Dr. M. Ketata and Prof. H. Hajji, République tunesienne, Ministère

de Transport, Institute National de la Météorologique, Tunis-Carthage. For Egypt, France, Hungary, Malta, Morocco, Portugal, Serbia, Syria and Turkey the data have been obtained from the GHCN (Global Historical Climatology Network) version 2 and/or where kindly provided by the German Meteorological Service (DWD), Geschäftsfeld Seeschifffahrt and David Lister, Climatic Research Unit, University of East Anglia, Norwich, UK. Tommaso Abrate, Department of Hydrology and Water Resources, WMO, Geneva, Switzerland, provided us with addresses and relevant information on how to contact the responsible persons and institutions from the different countries. Dr. J. Fidel González-Rouco was partially funded by project REN-2000-0786-cli and Dr. Jürg Luterbacher was supported by the Swiss NCCR Climate programme.

References

Barnett TP, Preisendorfer RW (1987) Origins and levels of monthly and seasonal forecast skill for United States air temperature determined by canonical correlation analysis. Mon Weather Rev 115:1825–1850

Barnston AG, Livezey RE (1987) Classification, seasonality and persistence of low frequency atmospheric circulation patterns. Mon Weather Rev 115:1083–1126

Bartzokas A, Metaxas DA, Ganas IS (1994) Spatial and temporal sea-surface temperature covariances in the Mediterranean. Int J Climatol 14:201–213

Brier GW (1950) Verification of forecasts expressed in terms of probability. Mon Weather Rev 78:1–3

Corte-Real J, Zhang X, Wang X (1995) Large-scale circulation regimes and surface climatic anomalies over the Mediterranean. Int J Climatol 15:1135–1150

Corte-Real J, Qian B, Xu H (1998) Regional climate change in Portugal: precipitation variability associated with large-scale atmospheric circulation. Int J Climatol 18:619–635

Cubasch U, Meehl GA, Boer GJ, Stouffer RJ, Dix M, Noda A, Senior CA, Raper S, Yap KS (2001) Projections of future climate change. In: Houghton JT, Ding Y, Griggs DJ, Noguer M, van der Linden PJ, Xiaoxu D (eds) Climate change 2001; the scientific basis, ch 9. Contribution of Working Group I to the Third Assessment Report of the Intergovernmental Panel on Climate Change (IPCC). Cambridge University Press, Cambridge, UK, pp 99–181

Dai A, Fung IY, del Genio AD (1997) Surface observed global land precipitation variations during 1900–1988. J Clim 10:2943–2962

Easterling DR, Karl TR, Gallo KP, Robinson TA, Trenberth KE, Dai AG (2000) Observed climate variability and change of relevance to the biosphere. J Geophys Res 105:20,101–20,114

Folland CK, Karl TP, Christy JR, Clarke RA, Gruza GV, Jouzel J, Mann ME, Oerlemans J, Salinger MJ, Wang SW (2001) Observed climate variability and change. In: Houghton JT, Ding Y, Griggs DJ, Noguer M, van der Linden PJ, Xiaoxu D (eds) Climate change 2001; the scientific basis, ch 2. Contribution of working group I to the third assessment report of the Intergovernmental Panel on Climate Change (IPCC). Cambridge University Press, Cambridge, UK, pp 99–181

Giles BD, Balafoutis C (1990) The Greek heatwaves of 1987 and 1988. Int J Climatol 10:505–517

Giles BD, Balafoutis C, Maheras P (1990) Too hot for comfort: the heat waves in Greece in 1987 and 1988. Int J Biometeorol 34:98–104

Giorgi F (2002a) Variability and trends of sub-continental scale surface climate in the twentieth century. Part I: Observations. Clim Dyn 18:675–691

Giorgi F (2002b) Variability and trends of sub-continental scale surface climate in the twentieth century. Part II: AOGCM simulations. Clim Dyn 18:693–708

González-Rouco JF, Heyen H, Zorita E, Valero F (2000) Agreement between observed rainfall trends and climate change simulations in Southern Europe. J Clim 13: 3057–3065

González-Rouco JF, Jimenez JL, Quesada V, Valero F (2001) Quality control and homogenization of monthly precipitation data in the southwest of Europe. J Clim 14:964–978

Hansen J, Ruedy R, Sato M, Imhoff M, Lawrence W, Easterling D, Peterson T, Karl T (2001) A closer look at United States and global surface temperature change. J Geophys Res 106:23,947–23,963

Hansen J, Ruedy R, Sato M, Lo K (2002) Global warming continues. Science 295:275

Hunt B, Gordon H (1988) The problem of naturally occurring drought. Clim Dyn 3:19–33

Hurrell JW (1995) Decadal trends in the North Atlantic Oscillation: regional temperatures and precipitation. Science 269:676–679

Hurrell JW, van Loon H (1997) Decadal variations in climate associated with the North Atlantic Oscillation. Clim Change 36:301–326

IPCC (2001) Climate change 2001: the scientific basis. In; Houghton JT, Ding Y, Griggs DJ, Noguer M, van der Linden PJ, Dai X, Maskell K, Johnson CA (eds.) Contribution of working group I to third assessment report of the intergovernmental panel on climate change. Cambridge University Press, Cambridge, UK

Jacobeit J (2000) Rezente Klimaentwicklung im Mittelmeerraum. Petermanns Geogr Mittl 144:22–33

Jacobeit J, Jönsson T, Bärring L, Beck C, Ekström M (2001) Zonal indices for Europe 1780–1995 and running correlations with temperature. Clim Change 48:219–241

Jenne RL (1975) Data sets for meteorological research. NCAR TN 1A-111

Jones PD, New M, Parker DE, Martin S, Rigor IG (1999) Surface air temperature and its changes over the past 150 years. Rev Geophys 37:173–199

Kalnay et al. (1996) The NCEP/NCAR 40-Year Reanalysis Project. Bull Am Meteorol Soc 77:437–471

Katsouyanni K, Pantazopoulu A, Touloumi G, Tselepidaki I, Moustris K, Asimakopoulos D, Poulopoulou G, Trichopoulos D (1993) Evidence of interaction between air pollution and high temperatures in the causation of excess mortality. Archit Environ Health 48:235–242

Katsouyanni K, Trichopoulos D, Zavitsanos X, Touloumi G (1988) The 1987 Athens heatwave. Lancet 573:ii

Kattenberg A, Giorgi F, Grassl H, Meehl GA, Mitchell JFB, Stouffer RJ, Tokioka T, Weaver AJ, Wigley TML (1996) Climate models – projections of future climate. In: Houghton JT, Meirho Filho LG, Callander BA, Harris N, Kattenberg A, Maskell K (eds) Climate Change 1995. The Science of Climate Change. The second assessment report of the IPCC contribution of WG1. Cambridge University Press, pp 285–357

Kistler R et al. (2001) The NCEP-NCAR 50-year Reanalysis: monthly means CD-ROM and documentation. Bull Am Meteorol Soc 82:247–267

Kundzewicz ZW, Parry ML (2001) Europe. In: McCarthy JJ, Canziani OF, Leary NA, Dokken DJ, White KS (eds) Climate change 2001. Impacts, adaptations and vulnerability. Contribution of working group II to the third Assessment report of the intergovernmental panel on climate change. Cambridge University Press, Cambridge, UK and NY, USA

Kutiel H, Maheras P (1998) Variations in the temperature regime across the Mediterranean during the last century and their relationship with circulation indices. Theor Appl Climatol 61:39–53

Kutiel H, Benaroch Y (2002) North Sea-Caspian pattern (NCP) – an upper level atmospheric teleconnection affecting the Eastern Mediterranean: identification and definition. Theor Appl Climatol 71:17–28

Livezey RE (1995) The evaluation of forecasts. In: von Storch H, Navarra A (eds.) Analysis of climate variability. Springer, Berlin, New York, Heidelberg, pp 177–196

Livezey RE, Smith TM (1999a) Considerations for use of the Barnett and Preisendorfer (1987) algorithm for canonical correlation analysis of climate variations. J Clim 12:303–305

Livezey RE, Smith TM (1999b) Covariability of aspects of North American climate with global sea surface temperatures on interannual to interdecadal timescales. J Clim 12:289–302
Lolis CJ, Bartzokas A, Metaxas DA (1999) Spatial covariability of the climatic parameters in the Greek area. Int J Climatol 19:185–196
Maheras P (2000) Synoptic situations causing drought in the Mediterranean basin. In: Vogt JV, Somma F (eds) Drought and drought mitigation in Europe. Kluwer Academic, Dardrecht, pp 91–102
Maheras P, Kutiel H (1999) Spatial and temporal variations in the temperature regime in the Mediterranean and their relationship with circulation; 1860–1990. Int J Climatol 19:1697–1715
Maheras P, Flocas HA, Patrikas I, Anagnostopoulou C (2001) A 40 year objective climatology of surface cyclones in the Mediterranean region: spatial and temporal distribution. Int J Climatol 21:109–130
Maheras P, Xoplaki E, Davies TD, Martin-Vide J, Barriendos M, Alcoforado MJ (1999) Warm and cold monthly anomalies across the Mediterranean basin and their relationship with circulation; 1860–1990. Int J Climatol 19:1697–1715
Matzarakis A, Mayer H (1991) The extreme heat wave in Athens in July 1987 from the point of view of human biometeorology. Atmos Env 25B:203–211
Matzarakis A, Mayer H (1997) Heat stress in Greece. Int J Biometeorol 41:34–39
Michaelsen J (1987) Cross-validation in statistical climate forecast models. J Climate Appl Meteorol 26:1589–1600
Namias J (1948) Evolution of monthly mean circulation and weather patterns. Trans Am Geophys U29:777–788
New MG, Hulme M, Jones PD (1999) Representing twentieth-century space time climate variability. Part I: development of a 1961–1990 mean monthly terrestrial climatology. J Clim 12:829–856
New MG, Hulme M, Jones PD (2000) Representing twentieth-century space time climate fields. Part II: development of a 1901–1996 mean monthly terrestrial climatology. J Clim 13:2217–2238
New M, Todd M, Hulme M, Jones P (2001) Precipitation measurements and trends in the twentieth century. Int J Climatol 21:1899–1922
Nicholls N, Gruza GV, Jouzel J, Karl TR, Ogallo LA, Parker DE (1996) Observed climate variability and change. In: Houghton JT, Meira Filho LG, Callander BA, Harris N, Kattenberg A, Maskell K (eds.) Climate change 1995; the science of climate change, ch 3. Contribution of working group I to the second assessment report of the Intergovernmental Panel on Climate Change (IPCC). Cambridge University Press, Cambridge, UK, pp 133–192
North GR, Moeng FJ, Bell TL, Cahalan RF (1982) The latitude dependence of the variance of zonally averaged quantities. Mon Weather Rev 110:319–326
Palutikof JP, Conte M, Casimiro Mendes J, Goodess CM, Esprito Santo F (1996) Climate and Climatic Change. In: Brandt CJ, Thornes JB (eds.) Mediterranean desertification and land use. Wiley, New York, pp 43–86
Perry AH (2001) More heat and drought – can Mediterranean tourism survive and prosper? In: Matzarakis A, de Freitas CR (eds) Proc 1st International workshop on climate, tourism and recreation. Int Soc Biometeorol, commission on climate tourism and recreation. December 2001, Thessaloniki, Greece, WP3, pp 1–6
Peterson TC, Vose RS (1997) An overview of the global historical climatology network temperature database. Bull Am Meteorol Soc 78:2837–2849
Peterson TC, Vose RS, Schmoyer R, Razuvaëv V (1998) Global historical climatology network (GHCN) quality control of monthly temperature data. Int J Climatol 18:1169–1179
Pozo-Vázquez D, Esteban-Parra MJ, Rodrigo FS, Castro-Diez Y (2001) A study of NAO variability and its possible non-linear influences on European surface temperature. Clim Dyn 17:701–715
Ratcliffe RAS (1978) Meteorological aspects of the 1975–76 drought. Proc R Soc London A 363:3–20
Rayner NA, Horton EB, Parker DE, Folland CK, Hackett RB (1996) Version 2.2 of the global sea-Ice and sea surface temperature data set, 1903–1994. CRTN 74. Available from Hadley Centre Met Office Bracknell, UK
Reddaway JM, Bigg GR (1996) Climatic change over the Mediterranean and links to the more general atmospheric circulation. Int J Climatol 16:651–661
Ribera P, Garcia R, Diaz HF, Gimeno L, Hernandez E (2000) Trends and interannual oscillations in the main sea-level surface pressure patterns over the Mediterranean, 1955–1990. Geophys Res Lett 8:1143–1146
Rimbu N, le Treut H, Janicot S, Boroneant C, Laurent C (2001) Decadal precipitation variability over Europe and its relation with surface atmospheric circulation and sea surface temperature. Q J R Meteorol Soc 127:315–329
Saenz J, Rodriguez-Puebla C, Fernandez J, Zubillaga J (2001) Interpretation of interannual winter temperature variations over southwestern Europe. J Geophys Res 106:20,641–20,651
Slonosky VC, Yiou P (2002) Does the NAO index represent zonal flow? The influence of the NAO on North Atlantic surface temperature. Clim Dyn 19:17–30
Slonosky VC, Jones PD, Davies TD (2001) Atmospheric circulation and surface temperature in Europe from the 18th century to 1995. Int J Climatol 21:63–75
Smith TM, Livezey RE (1999) GCM systematic error correction and specification of the seasonal mean Pacific-North America region atmosphere from global SSTs. J Clim 12:273–288
Trenberth KE (1990) Recent observed interdecadal climate changes in the Northern Hemisphere. Bull Am Meteorol Soc 71:989–993
Trenberth KE (1995) Atmospheric circulation climate changes. Clim Change 31:427–453
Trenberth K, Paolino DA (1980) The Northern Hemisphere sea-level pressure data set: trends, errors and discontinuities. Mon Weather Rev 108:855–872
Trigo IF, Davies TD, Bigg GR (1999) Objective climatology of cyclones in the Mediterranean Region. J Clim 12:1685–1696
Trigo IF, Davies TD, Bigg GR (2000) Decline in Mediterranean rainfall caused by weakening of Mediterranean cyclones. Geophys Res Lett 27:2913–2916
Tsiourtis NX (2001) Drought management plans for the Mediterranean region. Report of the Water Development Department, Nicosia, Cyprus. Available at: http://www.pio.gov.cy/wdd/eng/scientific_articles/archieve2001/article03.htm
von Storch H, Zwiers FW (1999) Statistical analysis in climate research. Cambridge University Press, UK
Vose RS, Schmoyer RL, Steurer PM, Peterson TC, Heim R, Karl TR, Eischeid J (1992) The Global Historical Climatology Network: long-term monthly temperature, precipitation, sea level pressure, and station pressure data. ORNL/CDIAC-53, NDP- 041, Carbon Dioxide Information Analysis Center, Oak Ridge National Laboratory, Oak Ridge, Tennessee, USA
Watson RT, Zinyowera RH, Moss H (1997) The regional impacts of climate change: an assessment of vulnerability. IPCC Spec Rep Working Group II. Cambridge University Press, UK
Wilks DS (1995) Statistical methods in the atmospheric sciences: an introduction. In: Dmowska R, Holton JR (eds.) Int Geophys Ser, 59. Academic Press, New York, USA
WMO (1986) Guidelines on the quality control of surface climatological data/prepared by Abbott PF (UK) as Rapporteur in the WMO Commission for Climatology. Geneva: WCP, (WCP-85). iv, appendices
Xoplaki E (2002) Climate variability over the Mediterranean. PhD thesis, University of Bern, Switzerland ([http://sinus.unibe.ch/klimet/docs/phd_xoplaki.pdf])
Xoplaki E, Luterbacher J, Burkard R, Patrikas I, Maheras P (2000) Connection between the large-scale 500 hPa geopotential height fields and precipitation over Greece during wintertime. Clim Res 14:129–146

Xoplaki E, González-Rouco FJ, Gyalistras D, Luterbacher J, Rickli R, Wanner H (2002) Interannual summer air temperature variability over Greece and its connection to the large-scale atmospheric circulation and Mediterranean SSTs 1950–1999. Clim Dyn DOI 10.1007/s00382-002-0291-3

Xu JS (1993) The joint modes of the coupled atmosphere–ocean system observed from 1967 to 1987. J Clim 6:816–838

Zorita E, von Storch H (1999) The analog method – a simple statistical downscaling technique: comparison with more complicated methods. J Clim 12:2474–2489

Zorita E, Kharin V, von Storch H (1992) The atmospheric circulation and sea surface temperature in the North Atlantic area in winter: their interaction and relevance for Iberian precipitation. J Clim 5:1097–1108